Evaluation of Multiloop Diagrams via Lightcone Integration

Y.J. Feng† and C. S. Lam*
Department of Physics, McGill University, 3600 University St., Montreal, P.Q., Canada H3A 2T8

We present a systematic method to determine the dominant regions of internal momenta contributing to any two-body high-energy near-forward scattering diagram. Such a knowledge is used to evaluate leading high-energy dependences of loop diagrams. It also gives a good idea where dominant multiparticle cross sections occur.

arXiv:hep-ph/9707396v2 3 May 1998

I. INTRODUCTION

It is difficult to compute high-energy ($\sqrt{s}$) scattering amplitudes at small momentum transfers ($\sqrt{-t}$), even assuming the coupling constant g^2 to be small. This is so because each loop of a Feynman diagram is capable of producing a $\ln s$ factor, thus changing the effective expansion parameter from g^2 to $g^2 \ln s$. Even though the former may be small, the latter can become quite sizable at high energies, necessitating diagrams of high orders to be included. Such is for example the case when total cross section is computed in the framework of QCD [1].

Usually such a daunting task of computed diagrams of many loops may be contemplated only in the leading-log approximation (LLA), though there are exceptions, especially for sets of diagrams with regular structures [2]. In LLA , only terms of the highest power of $\ln s$ are kept at each perturbative order, but even so the computation is far from being simple. For low-order diagrams, or diagrams with highly regular structures, the computation has been carried out and the results are well known [3–6]. However, for complicated diagrams, a systematic procedure to find even the leading-log contribution seems to be lacking. We shall discuss a method in the present paper. The available QCD result, via the exchange of the BFKL Pomeron [5], violates the Froissart bound and needs to be improved [8]. Other diagrams must be included to restore unitarity so it would be useful to have a way to find out how the other diagrams behave at high energies. This can be achieved if the regions of internal momenta dominating the Feynman amplitude can be located, for then one simply integrates around them to obtain the LLA result.

For quark-quark scattering via the exchange of gluon ladders, the dominant region is known to be the multi-Regge region [4,5], where gluons produced in the intermediate states are strongly ordered in rapidity, and the gluons being exchanged are dominantly spacelike. What we would like to discuss in the present paper is a general way to find such dominant regions for any diagram, and its associated high-energy dependence in LLA. We shall carry out the study for Feynman diagrams and for nonabelian cut diagrams [10–12], both because they are more general, and because there is already a considerable body of literature on the dispersion theoretic techniques [5,6].

Such calculations of elastic amplitudes, besides giving the energy-dependence of total cross-sections via the optical theorem [1], also tell us the kinematical regions where the dominant inelastic cross-sections come from, for via unitarity these are intimately related to the dominant internal momenta of the elastic amplitude. This knowledge would be of direct phenomenological interest as well.

The methods developed in this paper should also be useful in the study of two-dimensional effective QCD Lagrangians at high-energies [13,14]. A prerequisite needed to arrive at a reliable effective Lagrangian is to know which are the heavy modes that can be discarded, and which of them must be integrated out to yield a new vertex in the effective Lagrangian. In perturbative language this is equivalent to finding the important regions of internal momenta around which to integrate. All others may simply be discarded.

In the rest of this section we shall describe what our method is based on, and provide a brief summary of the results.

At high energies it is convenient to use lightcone coordinates, $k_\pm = k^0 \pm k^3$. The components of a four-vector k^μ can then be written as $(k_+, k_-, k_\perp)$, and the loop integration expressed as $d^4k = dk_+ dk_- d^2k_\perp/2$. In the centre-of-mass system, the momenta of the two incoming particles, with masses neglected, can be taken to be $p_2 = (\sqrt{s}, 0, 0)$ and $p_1 = (0, \sqrt{s}, 0)$. The momentum transfer $\sqrt{-t}$ as well as all other transverse momenta $k_\perp$ are taken to be of order 1 as $s \to \infty$, so it is only the dominant regions in k_+ and k_- for every loop momentum k that have to be determined.

These regions are determined in the following way. First, observe that the inverse of the internal propagators are bilinear in the '+' and the '−' components of their line momenta, so the propagators give rise to simple poles in the '+' (or the '−') momenta which enable integrations in those variables to be carried out exactly by residue calculus [4]. Once this is done the locations of the '+' momenta are determined by the locations of the contributing poles and the '−' momenta. The '−' momenta are then fixed to be in the regions yielding the leading-log contributions to the amplitude.

We shall be able to do this both for Feynman diagrams and 'nonabelian cut diagrams' [10–12]. Feynman diagrams are fundamental, but they often have the undesirable property that the LLA contributions of individual diagrams get cancelled in the sum [4]. To the extent that the usual technology only allows LLA to be computed, this cancellation is disastrous because it leaves no viable means to compute the leading high-energy behaviour of the sum. Nonabelian cut diagrams are designed to combat this problem. The cancellation is actually a result of the destructive interference between the virtual gluons being exchanged. The nonabelian cut diagrams allow the destructive interferences to take place before high energy approximations are taken. In this way the LLA contribution to the nonabelian cut diagrams will reflect directly the leading contributions to the sum. No further cancellation will occur.

In Sec. 2 we will review the *flow diagram* method of Cheng and Wu [4] for carrying out the '+' component integrations by residue calculus. This method is very effective in locating the poles and the dominant integration regions for relatively simple diagrams. In complicated diagrams one encounters the problem of *flow reversal* which will be discussed in Sec. 3. This problem prevents a simple reading of the contributing poles directly from the flow diagrams. Nevertheless the locations of these poles can still be computed, but the complexity of computation grows quite fast with the number of loops of the diagram. This difficulty is then overcome by a 'path' method to be discussed in Sec. 4. With this mehtod the contributing poles can be located and the '+' momenta determined. What remains is to find the dominant '−' momenta that give rise to the LLA contribution. The recipe for doing so will be discussed in Sec. 5. Finally, in Sec. 6, a number of examples are given to illustrate the procedure.

II. FLOW DIAGRAMS

Consider a diagram with n internal lines and ℓ loops, whose line and loop momenta are denoted by q_i $(1 \le i \le n)$ and k_b $(1 \le b \le \ell)$ respectively. In lightcone coordinates, the denominator of the propagator for a line with momentum q is $d(q) = (q^2 - m^2 + i\epsilon) = (q_+q_- - q_\perp^2 - m^2 + i\epsilon) \equiv (q_+q_- - a + i\epsilon)$. These n propagators collectively define a set of poles for the integration variables k_{b+}, thus enabling these integrations to be performed with the help of residue calculus. To carry out this program we must identify, for each k_{b+}, which are the poles in the upper-half plane and which are the poles in the lower-half plane, for only the poles in one half-plane will be picked up by a contour integration. Their locations in turn depends on the sign of q_{i-}, the choice of loop momenta, as well as the order the k_{b+} integrations are carried out. With so many variables the problem is very complex indeed. *Flow diagram* was invented [4] to keep track of things and to determine the location of poles. We shall review its essence [4] in this section, and point out in the next section some of the complications hitherto overlooked. This complication makes it complicated to apply it to multiloop diagrams. In Sec. 4 we shall propose a *'path method'* to bypass these complications, and enables the evaluation of the '+' integration to be carried out in a simple manner.

A flow diagram is a Feynman diagram (or a nonabelian cut diagram) with arrows attached to each of its internal lines to indicate the direction of q_{i-}. Since the signs of the q_-'s vary over the integration region, generally more than one flow diagram is present for each Feynman or nonabelian cut diagram. Nevertheless, for a diagram with n internal lines, there are far fewer than 2^n flow diagrams that one might otherwise expect, for two reasons. First, momentum conservation forbids the arrows from a common vertex to point all inwards or all outwards. Secondly, for reasons to be explained below, one can reject flow diagrams in which arrows around any closed loop all point in the same (clockwise or counter-clockwise) direction. With these two requirements, it is easy to see that the 1-loop box diagram has only one flow diagram, rather than $2^4 = 16$.

In a flow diagram the signs of q_{i-} along the arrows are all positive, by definition. This allows the positions of the poles be located and the '+' integrations to be carried out, once the independent loops and their order of integrations are chosen. We shall now proceed to see how this is accomplished for the first integration, say k_{1+}.

k_{1+} flows through the lines of this first loop either in a clockwise or a counter-clockwise direction. Its coefficient in $d(q_i)$ is $\pm q_{i-}$, depending on whether this direction is the same as the arrow or opposite. The pole of $1/d(q_i)$ in k_{1+} has an imaginary part $\mp i\epsilon/q_{i-}$, with all $q_{i-} > 0$ by definition. Hence the lines with arrows pointing one way (clockwise or counter-clockwise) have poles all in one half-plane, and those with arrows pointing the opposite way have poles in the other half-plane. Which is which does not matter because we can always define the loop momentum by reversing its sign.

It is now easy to understand the assertion made earlier in the section, that flow diagrams containing a closed loop with flow arrows all pointing in the same direction may be rejected. Taking this loop as the first loop of integration, this would imply all poles to be in the same half-plane. By closing the integration contour in the other half-plane, we get a zero integral so such a flow diagram can be ignored.

Sometimes pole locations for *subsequent integrations* can be located in the same way, *i.e.,* by the direction of arrows in the flow diagram. In fact the explicit examples shown in Ref. [4] all seem to be of this type.

However, it is not guaranteed that pole locations for subsequent integrations can be located this way, as we shall now see. This is the complication mentioned in the section.

To make it easier to describe things later on, we shall call two momenta pointing in the same (opposite) direction around a loop to be *parallel (anti-parallel)* in that loop.

III. FLOW REVERSAL

Suppose there are n_1 poles picked up by the k_{1+} integration, each contributing to a term in the integral. As a result of the integration, k_{1+} acquires an imaginary part $\mp i\epsilon/q_{i-}$ from the ith pole. The sign is $-/+$ if k_{1+} and q_{i-} are parallel/anti-parallel. This imaginary part in turn imparts an imaginary part on every q_{j+} of the first loop, which is why the location of poles for the second and subsequent integrations may be altered. For simplicity, we shall assume from now on that ϵ is finite and positive, and has a common value in all the propagators.

This imaginary part of k_{1+} affects the location of poles in subseqent integrations only for lines j lying in loop 1. In that case, the imaginary part of $d(q_j)$ is changed from $i\epsilon$ to $i\epsilon(\mp q_{j-}/q_{i-}+1)$, with sign $-/+$ when lines j and i are parallel/anti-parallel in loop 1. Unless the sign is $-$ and $q_j > q_i$, the imaginary part of $d(q_j)$ remains positive and the location of pole j in subsequent integrations is once again determined solely by the direction of its arrow around the integration loop, *viz.,* it can be determined directly from the flow diagram. However, if lines j and i are parallel in the first loop, and that $q_j > q_i$, then the sign of the imaginary part of $d(q_j)$ becomes negative, and the pole location (upper or lower plane) will now be opposite to naive expectations from the flow diagram. This situation can still be accommodated into the flow diagram if we simply reverse the arrow of this line by hand. This is *flow reversal*.

To summarize, here is how poles for the '+' integrations are computed for a given flow diagram, assuming a set of independent loops and a given order of k_{b+}-integrations have been chosen.

For the first loop, use the *naive rule* to read it off the flow diagram. This means that lines of this loop with arrows pointing in the same direction have their poles in the same half plane.

Assuming now k_{b+}-integrations have been carried out for $b = 1, 2, \cdots, c$. We shall now proceed to do the $(c+1)$th integration for the term resulting from picking up poles located at line i_b for the bth loop, $b = 1, 2, \cdots, c$.

First note that whatever loop $(c+1)$ is, it should not contain any of the lines $i_1, i_2, \cdots, i_c$. This is because the '+' momenta of these lines have been determined by previous integrations so they cannot be fixed again by the $(c+1)$th integration.

The naive rule can be used for lines j in loop $(c+1)$ if, (i) it is not in any one of the previous loops, $1, 2, \cdots, c$, (ii) it is in a previous loop b but j is anti-parallel to i_b in that loop, or (iii) j is parallel to i_b around loop b but $q_{j-} < q_{i_b-}$. In the remaining case, when j and i_b are parallel in loop b but $q_{j-} > q_{i_b-}$, we must reverse the arrow direction of line j before the naive rule is applied.

After all ℓ '+'-integrations are carried out, we obtain a number of terms, each of which is specified by a set of poles i_b for loop b. We shall call this collection of lines, $I = (i_1 i_2 \cdots i_\ell)$, a *contributing pole*.

Let us illustrate this recipe of obtaining contributing poles with two explicit examples: a two-loop diagram, and a four-loop diagram. In the process we will see how important it is to take flow reversals into account just to maintain consistency.

A. A two-loop example

Fig. 1 is one of two possible flow diagrams for a two-loop Feynman diagram; the other has line 6 reversed.

Let a denote the loop with lines (1536) and b the loop with lines (2647). The big loop with lines (153472) is the union of these two loops and will be denoted by $a.b$. Only two of the three loop-momenta are independent.

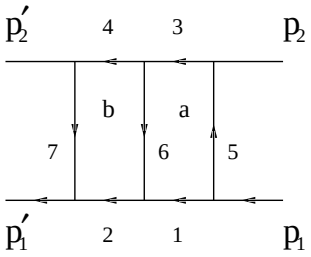

FIG. 1. A two-loop (Feynman) flow diagram.

There are three ways to start out the first loop integration, but the final results of their integrals must be the identical, and we must be able to pick the same contributing poles as well. We will illustrate here in detail how the latter can be achieved, *iff* proper flow reversals are taken into account.

Suppose we first integrate over loop a. In this loop the arrow of line 1 and the arrows of lines 5,3,6 are opposite, so their respective poles lie in opposite half planes of k_{a+}. We shall pick line 1 to be the relevant pole for further discussions. To simplify later descriptions we shall abbreviate this process of picking pole 1 from loop a simply by $a(1)$.

Now we are ready to tackle the second integration. Since line 1 is on $a.b$ we must not choose $a.b$ to be the second loop, so we are forced to choose it to be b. Line 6, which is in both loops b and a, is anti-parallel to line 1 in loop a, so the naive rule once again applies to loop b. Lines 6 and 2 are on one half-plane, and lines 4 and 7 on the other. We shall pick 2 and 6 to be the relevant poles. Consequently, we obtain two contributing poles, $I_1 = (1, 2)$ from $a(1)b(2)$, and $I_2 = (1, 6)$ from $a(1)b(6)$.

Next, let us start all over again but this time first carry out the integration around loop b to get $b(2)$ and $b(6)$. Now since line 2 lies in $a.b$, for the term $b(2)$ the second loop must be chosen to be a. In loop b line 6 is parallel to line 2, so there is a chance it might suffer a flow reversal. However, since $q_{2-} = q_{6-} + q_{1-} > q_{6-}$, flow reversal does not occur. Hence we have $b(2)a(1)$, so this contributing pole is $I_1 = (1, 2)$. For the term $b(6)$, since 6 is in a, the second loop must be chosen to be $a.b$. Now lines 2,4,7 are all in the first loop b, but 4 and 7 will not suffer flow reversal because they are antiparallel to 6. Line 2 is a different matter since $q_{2-} > q_{6-}$, so it would suffer a flow reversal. With this reversal, all lines in $a.b$ point in the same direction, with the sole exception of 1, so this yields $b(6)a.b(1)$, and the contributing pole is $I_2 = (1, 6)$. In this way we obtain the same set of contributing pole as before, as we should.

Finally suppose we carry out $a.b$ first, getting two terms $a.b(1)$ and $a.b(2)$. In the first case line 1 is in a so the second loop must be b. Lines 4 and 7 in b are antiparallel to 1 so they do not suffer from flow reversal. Line 2 is parallel to 1 and $q_{2-} > q_{1-}$ so it does suffer a flow reversal, thus leaving behind only line 6 of loop b in one direction. From $a.b(1)$ we therefore obtain $a.b(1)b(6)$ and the contributing pole $I_2 = (1, 6)$. Now consider the term $a.b(2)$. The second loop must now be a. Lines 5, 3 are antiparallel to 2 so they do not suffer flow reversal. Line 1 is parallel to 2 but $q_{1-} < q_{2-}$, so it does not suffer from flow reversal either. So no flow reversal occurs at all for lines in loop a, and this term yields $a.b(2)a(1)$, giving rise to the contributing pole $I_1 = (1, 2)$. The result is once again the same as the other two calculations. If flow reversals were not properly taken into account, the result would have been different and wrong.

The main lesson learned from this very simple example is that generally detailed loop-by-loop calculation must be performed, with proper flow reversals taken into account, in order to obtain the correct locations of the contributing poles. Also, the amount of calculations needed to determine the contributing poles may depend critically on the independent loops chosen and the order of integrations performed.

B. A four-loop example

The task of obtaining the contributing poles becomes more arduous for diagrams with a larger number of loops. The calculation must be carried out loop by loop, with more and more terms and flow reversals to keep track of. Besides, with multiloops there is a huge number of ways in choosing the independent loops and their order of integrations, each giving very different intermediate results though at the end they must all yield the same contributing poles. It is not known a priori how to make the best choice to maximally simplify the intermediate calculations.

To illustrate these points we shall work out in this subsection a four-loop example and obtain its contributing poles in two different ways.

Consider Fig. 2, with the following choice of independent loops: $a = (4, 8, 12, 13, 7)$, $b = (5, 9, 3, 11, 12, 8), c = (13, 12, 10, 1, 6)$, and $d = (10, 12, 11, 2)$. Note that lines 8 and 13 are supposed not to intersect in the diagram. We shall carry out the integrations in the order a, b, c, d as much as possible.

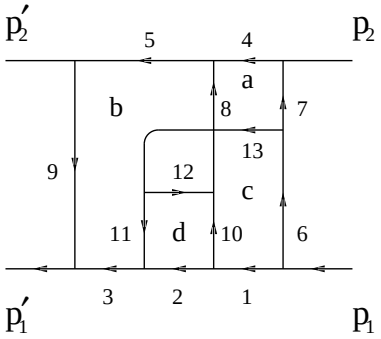

FIG. 2. A four-loop (Feynman) flow diagram.

The first integration over loop a yields $a(4)$ and $a(7)$.

We do the b integration next. The only lines common to loops a and b are 8 and 12, but since they are antiparallel to 4 and 7, no flow reversal takes place in carrying out the b integration. After the b-integration we get four terms, which for brevity shall be written together as additions: $[a(4) + a(7)][b(3) + b(11)]$.

Line 12 of loop c is also in loop a and loop b, and line 13 of loop c is in loop a. Since line 12 is antiparallel to 4 and 7 in loop a, and antiparallel to 3 and 11 in loop b, it suffers no flow reversal at loop c. Similarly line 13, being antiparallel to lines 4 and 7 in loop a, also has no flow reversal. Thus after the c integration, we get $[a(4) + a(7)][b(3) + b(1)][c(1) + c(10)]$.

The final d-integration is a bit complicated because loop d contains some of these poles from previously integrations so we are sometimes forced to take the loop $d.c$ or the loop $d.b$ instead of d itself. The final result contains 10 terms:

$$\begin{aligned}
&[a(4) + a(7)]b(3)c(1)[d(10) + d(11)] + \\
&[a(4) + a(7)]b(3)c(10)d.c(2) + \\
&[a(4) + a(7)]b(11)[c(1)d.b(2) + c(10)d.c(2)].
\end{aligned} \tag{3.1}$$

To summarize, we have obtained ten contributing poles: (7,3,1,10), (7,3,1,11), (7,3,10,2), (7,11,2,1), (7,11,2,10), as well as another five with line 7 replaced by line 4.

Let us now illustrate another way to get the same result, by choosing this time the four independent loops to be $a = (4, 8, 12, 13, 7), b = (5, 9, 3, 11, 12, 8)$, $e = c.d = (1, 6, 13, 11, 2)$, and $d = (10, 12, 11, 2)$, and try to carry out the integration in the order $a, b, c.d, d$ as much as possible.

These loops are what we shall later call the *natural loops* for the contributing pole (7,3,1,10). They are obtained first by removing the lines 7,3,1,10 from the original diagram, and then inserting one of them back at a time to get the four loops.

The first two integrations are identical to those before, so we get $[a(4) + a(7)][b(3) + b(11)]$. Now $e = c.d$ contains the line 11 but not 3, so the next integration involving $b(3)$ gives $e(1) + e(2)$ but the next integration involving $b(11)$ gives $c(1) + c(10)$, as $c = d.(c.d)$. The last loop d contains lines 2 and 11, so for some terms the integration over d has to be changed into integration over $d.b$ or $d.e = c$. The final answer is

$$\begin{aligned}
&[a(4) + a(7)]b(3)e(1)[d(10) + d(11)] + \\
&b(3)e(2)c(10) + b(11)c(1)d.b(2) + \\
&b(11|3)c(10)d.b(2).
\end{aligned} \tag{3.2}$$

This results in the same ten contributing poles as before, as it should.

The calculation could be even more complicated if we encounter a line j which is parallel to a pole line i of an earlier loop, but the relative magnitude of q_{j-} and q_{i-} can be either way. In that situation we must divide this flow

diagram into two, one in which $q_{j-} < q_{i-}$ and line j is not reversed, and the other with $q_{j-} > q_{i-}$ where line j must be reversed.

IV. PATH METHOD FOR FINDING CONTRIBUTING POLES

In this section we propose a simple (path-) method to obtain the contributing poles. With this method there is no need to declare the independent loops and their order of integrations, so there is no need to keep track of the complicated flow reversals either. This makes the method most useful in the presence of a large number of loops.

We begin by choosing a path P in the flow diagram. By a path we mean a continuous line (no branches, no loops) running from beginning to end, with all the arrows on it pointing in the same direction. The thin solid lines in Figs. 3 and 4 are examples of such paths. By adding branches to the path we can construct trees. A class of these trees, $T[P]$, turns out to be in one-one correspondence with the contributing poles. The path method of finding contributing poles is actually a method to construct the trees in $T[P]$.

From an ℓ-loop diagram one can obtain trees by removing ℓ lines. We shall refer to these removed lines as the *missing lines* for the tree. The set of all trees so obtained with path P as their common backbone will be denoted by $S[P]$. From $S[P]$ we select a subset $T[P]$ satisfying the following *directional rule*: when any one of the ℓ missing lines is inserted into the tree, a loop is formed. If the inserted line around this loop is parallel to the lines along path P, this tree is rejected. If it is anti-parallel, then this tree is retained to be a member of $T[P]$.

We assert that the missing lines of any tree in $T[P]$ is a contributing pole of the diagram, and there is actually a one-one correspondence between contributing poles and individual trees in $T[P]$. This is the essence of the *path method*.

This method does not restrict what path P one chooses, but the longer the path the fewer the number of contributing poles, and the easier the calculations. So in practice we often choose the longest path we can manage, though this is not a requirement of the method. In Sec. VIIC an example will be shown in which computations based on two different paths are shown for comparison. The reason why one can get the same result by choosing different paths P, or equivalently different sets of contributing poles, is because of the freedom to choose poles from either half-plane each time we carry out any integration.

We have implicitly assumed in these discussions that a path P is chosen after we are given a flow diagram. This is not strictly necessary. We may start from a Feynman diagram or a nonabelian cut diagram, without arrows attached, and start drawing a path on it. This can be taken as the starting point to determine possible flow diagrams consistent with this path: arrows on the path must all point in one direction, other arrows must be installed not to violate the direction rule to obtain contributing poles.

Before proceeding to prove the path method let us first see how it can be applied to obtain the contributing poles of Figs. 1 and 2 very simply.

A. Examples

For Fig. 1 let us choose the path P to be (5347), shown in Fig. 3 as thin solid lines. Then $S[P] = \{(P,6),(P,1),(P,2)\}$, and $T[P] = \{(P,6),(P,2)\}$. The tree $(P,1)$ violates the directional rule for the following reason so it is not in $T[P]$. When line 6 is inserted into $(P,1)$, it is parallel to P in the loop (6153), so it has to be rejected. With this $T[P]$, the contributing poles are the missing lines so they are (1,2) and (1,6), agreeing with the result obtained previously.

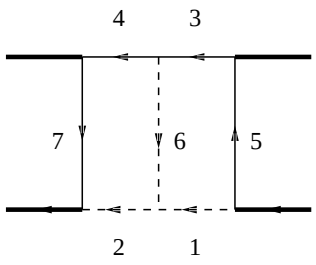

FIG. 3. The solid line is the path P used to obtain contributing poles for Fig. 1.

Let us next apply the method to obtain the contributing poles of Fig. 2, taking $P = (6, 13, 12, 8, 5, 9)$ as the path (Fig. 4). Then

$$T[P] = \{(P, 7, 2, 11), (P, 7, 2, 10), (P, 7, 1, 11), \\ (P, 7, 3, 10), (P, 7, 1, 3)\} ,$$

and five more with 7 replaced by 4. The contributing poles are therefore (7,3,1,10), (7,3,1,11), (7,3,10,2), (7,11,2,1), and (7,11,2,10), and another five with 7 replaced by 4, the same 10 terms as before. The trees in $S[P]/T[P]$ are $\{(P, 7, 1, 2), (P, 7, 2, 3), (P, 7, 10, 11)\}$, and three more with 7 replaced by 4. $(P, 7, 1, 2)$ violates the directional rule when the line 11 is inserted; $(P, 7, 2, 4)$ violates the directional rule when line 10 is inserted; and $(P, 7, 10, 11)$ violates the directional rule when 2 is inserted.

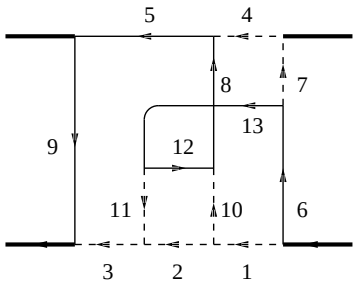

FIG. 4. The solid line is the path P used to obtain the contributing poles of Fig. 2.

B. Proof

A tree $t \in S[P]$ defines a set of independent loops $\mathcal{N}[t]$ of the original diagram by filling in the missing lines one at a time. The special feature of $\mathcal{N}[t]$ is that the missing lines are never on the boundary of two loops. We shall later on refer to these loops as the *natural loops* for the missing lines.

Now we proceed to the proof of the path method. We assume we always close the integration contour in the half-plane in which poles reside on lines running in the opposite direction as those on P.

The proof makes use of the simple fact that the same set of contributing poles can be computed using any independent loops and any order of integration.

Removing the pole lines of a contributing pole from the original diagram gives rise to a tree in $S[P]$. We shall denote the set of all such tress as $T'[P]$. Our task is to show that $T[P] = T'[P]$.

Take any $t' \in T'[P]$. The removed pole lines clearly satisfy the directional rule when they are inserted back, because poles are always taken from those lines running in the opposite direction as P. Hence $t' \in T[P]$ and $T'[P] \subset T[P]$.

Conversely, take a $t \in T[P]$, and use the independent loops $\mathcal{N}[t]$ to compute the contributing poles. The missing lines of t are obviously one of the pole lines, for according to the directional rule they all run opposite to the path direction. Hence $t \in T'[P]$ and $T[P] \subset T'[P]$.

Putting the two together, we get $T[P] = T'[P]$, as desired.

V. NONABELIAN CUT DIAGRAMS

General methods found in the literature to compute high energy limits of Feynman diagrams [3,4] are by and large valid only in the leading-log approximation (LLA). They become virtually powerless if these leading-log contributions cancel when the Feynman diagrams are summed, a situation which unfortunately occurs quite frequently [4]. A method was developed recently to bypass this difficulty, by allowing the cancellations to occur before the high energy limit is taken. The cancellations are incorporated into the individual *nonabelian cut diagrams* [10,12], whose spacetime amplitudes (for onshell diagrams) turn out to differ from the corresponding Feynman diagram only by having the denominators $(q_i^2 - m^2 + i\epsilon)^{-1}$ of certain propagators replaced by the corresponding Cutkosky propagators $-2\pi i\delta(q_i^2 - m^2)$. The advantage of the nonabelian cut diagrams is that the sum of Feynman diagrams is the same as the sum of nonabelian cut diagrams, but in the latter cancellations took place before the high-energy limit is taken, so their leading-log contributions (LLA) survive the sum. For this to happen it is clearly necessary for the LLA of a nonabelian cut digaram to have a smaller $\ln s$ power than the corresponding Feynman diagram, if the sum of the LLA contributions of the latter is to vanish. This is actually made possible by the presence of the Cutkosky propagators.

For high-energy two-body (*e.g., quark-quark*) scattering, the Cutkosky propagators occur only on the top quark lines. In the high energy limit, it can be shown that the combination $q_i^2 - m^2$ is actually proportional to the '$-$' momentum on that line, so a δ-function is that variable is a δ-function of the '$-$' momentum [10,11]. This has the effect of stopping the '$-$' momentum from flowing through this line, so as far as the flow diagram is concerned we may think of these lines as being absent. For the rest of the nonabelian cut diagram the flows are constructed in exactly the same way as in a Feynman diagram, and contributing poles can be located the same way just as well.

As an example, consider the nonabelian-cut (flow) diagram of Fig. 5, where the Cutkosky propagator is located at line 8, indicated there by a vertical bar (|). Hence the '$-$' momentum is absent from lines 8, and also from line 4 by continuity. We may therefore ignore these two lines in the rest of the discussions.

To obtain the contributing poles from the path method, we can choose the path to be $P = (1, 5, 10, 6, 3)$, then $T[P] = \{(P, 9), (P, 7)\}$, giving rise to the contributing poles (2,7) and (2,9).

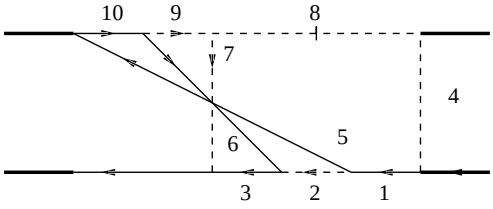

FIG. 5. A 3-loop (non-abelian cut) flow diagram. The solid line represents the path P.

VI. DOMINANT INTEGRATION REGIONS IN LLA

Contributing poles, extracted from the path method or otherwise, can be used to determine the internal momenta most important to the loop amplitude. The '$+$' momenta from the lines of a contributing pole $I = (i_1 i_2 \cdots i_\ell)$ are fixed by the pole condition to be $q_{i_k +} = (a_{i_k} - i\epsilon)/q_{i_k -}$, and those of any other line are fixed by momentum conservation. An easy way to read them out is to use the *natural loops* discussed before. These are simply the independent loops containing one and only one pole line each.

In LLA a number of simplifications emerge immediately. For quark-quark scattering in the c.m. system, quark 1 carries a '$-$' momentum $\sqrt{s}$ and quark 2 carries a '$+$' momentum $\sqrt{s}$. In LLA, where $|t|$ and squared masses are ignored compared to s, both quarks go straight through by carrying the full forward momenta with them. In other words, $q_{j-} \simeq \sqrt{s}$ for every line j of quark 1 (the 'bottom lines'), and $q_{j+} \simeq \sqrt{s}$ for every line j of quark 2 (the 'top lines'). This means that we can ignore the contributing poles with a pole line on top, for q_{j+} of a top line is $\sqrt{s}$ and

not determined by the pole condition above. In other words, if we insist on taking a pole there, then this term will not contribute in the LLA.

The two-body amplitude for a flow diagram, after the '+' integration is performed, can be written as

$$M = \int \left(\prod_{b=1}^{\ell} d^2 k_{b\perp} \right) F,$$
$$F = \int_R \left(\prod_{b=1}^{\ell} dx_b \right) G,$$
$$G \equiv \frac{N}{D} \equiv \frac{N}{\prod_{j=1}^{n} d_j}, \tag{6.1}$$

where $x_b = k_{b-}/\sqrt{s}$ and $Q_j = q_{j-}/\sqrt{s}$ are the scaled '$-$' momenta. In practice x_b are chosen from the Q_j's of types (i) and (ii) below. The integration region R of x_b is determined by the n flow-diagram conditions $Q_j \geq 0$.

The denominator $D = \prod_j d_j$ is derived from the denominators of the propagators $1/d(q_i)$, scaled in some convenient way as follows. (i) If line $j = i_k$ is part of the contributing pole I, then d_j is defined to be the scaled residue Q_j; (ii) if line j is a top line, then $d_j \equiv d(q_j)/s = \pm Q_j - a_j/s + i\epsilon \simeq \pm Q_j + i\epsilon$, where the sign in front of Q_j is $+/-$ if the arrow on line j is parallel/antiparallel to the '+' flow of quark 2; (iii) for any other line j, d_j is equal to $d(q_j)$ evaluated at the contributing pole, so

$$d_j = Q_j \sum \left(\pm \frac{a_{i_k}}{Q_{i_k}} \right) - a_j, \tag{6.2}$$

where the sum is taken over lines i_k in the same natural loops as line j, with an appropriate sign.

For convenience we will label lines of these three types by different indices: index p (for '*p*ole') for type (i), t (for '*t*op') for type (ii), and s (for '*s*ide') for type (iii). We shall retain the index j to denote any of them in general.

The numerator factor N consists of all the rest, including the vertex factors and factors of $\sqrt{s}$ discarded by D.

It should be noted that there are no explicit factors of 'i' hidden in M, except those explicity contained in the vertices and those appearing as $i\epsilon$ in the propagators. An ℓ-loop Feynman diagram has an explicit factor $(-i)^\ell$, and this is cancelled by the ℓ factors of $2\pi i$ from contour integration, leaving behind no explicit factors of i. This observation is important in determining how the imaginary part of a scattering amplitude arises.

For nonabelian cut diagrams with c cuts, the Feynman propagator $1/d(q)$ at each cut line is replaced by the Cutkosky propagators $-2\pi i\delta(q^2 - m^2)$ [10,11], so an explicit factor $(-i)^c$ will emerge.

From (6.1) and the rules for d_j, it would appear that the integral F diverges at the boundaries $Q_p = 0$ and $Q_t = 0$. Actually because of *obstructions* from the side lines s, the singularity in the Q_p variable is cancelled so there are no divergences at $Q_p = 0$. This is so because as $Q_p \to 0$, the '+' momentum $q_{p+} \simeq a_p/Q_p$ becomes very large. At some point it will become much smaller than all the Q_s, whence $d_s \simeq (Q_s/Q_p)a_s$ for any line s in the natural loop of p. This washes out the factor Q_p in d_p, leaving behind no divergence at this boundary.

A divergence does occur at $Q_t = 0$, but this divergence is an artifact of our high-energy approximation of dropping $\xi/s \equiv \mp(a_t - i\epsilon)/s$ compared Q_t, where ξ is of the order of the squared masses and the squared momentum transfer $-t$. If we restore it by installing a cutoff ξ/s at these boundaries, the divergences will be absent and they will be turned into enhancement factors of s. If the enhancement is logarithmic, the value of ξ does not matter in the LLA, and that will be the case in gauge theories. But if it is power-like, then the coefficient of the power dependence would depend on $\xi = \mp(a_t - i\epsilon)$, and its effective value could be determined only after the transverse-momentum integrations.

The integral F, thus enhanced, receives contributions in the form

$$F \simeq \int_{(\xi/s)} \frac{dQ_1'}{Q_1'^{m_1}} F_1, \tag{6.3}$$

where Q_1' is either one of the Q_t's, or the radial variable of several of them that are linearly independent. As it will become clear shortly this will be the smallest of all the '$-$' variables in the dominant integration region R_0.

In the region $Q_1' \ll Q_p$, we may set the ratios $Q_1'/Q_p = 0$ in all remaining d_s. This removes obstructions from some of the side lines, so that the integrand of F_1 may now encounter singularity again in some variable Q_2', say like $1/Q_2'^{m_2}$, with $m_2 \geq 1$. This new singular variable Q_2' would be equal to some Q_t or Q_p, or the radial variable of several of them. Now we have

$$F_1 \simeq \int_{B_1 Q_1'} \frac{dQ_2'}{Q_2'^{m_2}} F_2, \tag{6.4}$$

for some $B_1 \gg 1$. Similarly, in the region $Q_1' \ll Q_2' \ll Q_p$ for the remaining pole lines p, Q_2'/Q_p can also be set equal to zero, thus removing further obstructions from even more side lines. This enables another singular variable Q_3' to emerge, and so on. Continue this way until no further singularities are encountered, we get

$$F \simeq \int_{(\xi/s)} \frac{dQ_1'}{Q_1'^{m_1}} \int_{B_1 Q_1'} \frac{dQ_2'}{Q_2'^{m_2}} \int \cdots \int_{B_{v-1} Q_{v-1}'} \frac{dQ_v'}{Q_v'^{m_v}} F_{v+1}. \tag{6.5}$$

The integrand F_{v+1} is assumed to be regular so its Q_i' dependences can all be put equal to zero. All $B_i \gg 1$.

The dominant region of integration R_0 is then given by

$$R_0 = \{\xi/s \le Q_1' \ll Q_2' \ll \cdots \ll Q_v' \ll 1\}, \tag{6.6}$$

from which we can work out where the '+' momenta are located as well. The transverse momenta $k_{b\perp}$ are all of the same order as the momentum transfer $\sqrt{-t}$.

In gauge theories only logarithmic enhancements occur. This means all $m_i = 1$, and

$$F \simeq \frac{F_{v+1}}{v!} (\ln s)^v. \tag{6.7}$$

For an ℓ-loop Feynman diagram, the maximum enhancement is $\sim (\ln s)^\ell$. For an ℓ-loop nonabelian cut diagrams with c cuts, the maximum enhancement is $\sim (\ln s)^{\ell - c}$. We shall refer to diagrams with these maximal enhancements as *saturated*, and these are the diagrams of most interestes to us in LLA. Diagrams with less enhancements will be called *unsaturated*. A number of saturated and unsaturated diagrams are considered in the next section as concrete examples to illustrate the procedures here. For saturated diagrams we will also work out the coefficient of the leading-log term.

VII. EXAMPLES

A. Scalar Ladder Diagram

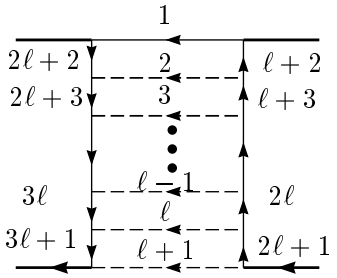

FIG. 6. Ladder diagram for scalar quarks and gluons. The path P is indicated by the light solid line and the poles indicated by the dotted lines. There is only one flow diagram and one contributing pole in this case.

Consider the ladder diagram Fig. 6 for scalar quarks and scalar gluons. There is only one non-zero flow diagram, as shown, and in it there is only one contributing pole, namely $I = (2, 3, \cdots, \ell + 1)$, indicated by the dotted lines. The path P from which this contributing pole is obtained is drawn as a light solid line in the diagram.

In the language of the last section, the pole lines are $2 \le p \le \ell + 1$, the top line is $t = 1$, and the side lines are $\ell + 2 \le s \le 3\ell + 1$.

The independent '+' momenta at the pole lines are given by

$$q_{p+}\sqrt{s} = (a_p - i\epsilon)/Q_p, \tag{7.1}$$

with $Q_{\ell+1} \simeq 1$ in LLA because it is a bottom line. Thus all these '+' momenta except $q_{\ell+1}$ are capable of being large if the corresponding Q_p is small enough. The '+' momenta carried by the side lines can most easily be read off from the natural loops, which are rectangles bounded below by the line p and bounded above by the top line 1.

Following the discussions of last section, the top line 1 is the unique candidate for the first singular variable Q'_1, and indeed it is with $m_1 = 1$. In the region $Q'_1 \ll Q_j$ for $j > 1$, obstructions from lines $\ell + 2$ and $2\ell + 2$ are removed, resulting in $d_{\ell+2} = -a_{\ell+2}$ and $d_{2\ell+2} = -a_{2\ell+2}$. This allows a new singular structure to emerge with $Q'_2 = Q_2$ and $m_2 = 1$. This in turn removes the obstruction from lines $\ell + 3$ and $2\ell + 3$ in the region $Q'_1 \ll Q'_2 \ll Q_j$ for $j > 2$, etc. Continuing this way, we obtain $Q'_j = Q_j$ and $m_j = 1$ for $1 \le j \le \ell$. Thus the diagram is saturated, and we obtain the amplitude to be

$$F = \frac{1}{\ell!}(\ln s)^\ell \prod_{i=\ell+2}^{3\ell+1} (-a_i). \tag{7.2}$$

In obtaining this expression, we have set the numerator N of the integrand to be 1.

The integration region is given by $R_0 = \{\xi/s \le Q_1 \ll Q_2 \ll \cdots \ll Q_\ell \ll 1\}$. According to (7.1), the '+' momenta are strongly ordered in the opposite way because the a_p's are all of the same order. The virtualities of the side lines s are all spacelike and of order 1, $q_s^2 = -a_s = -q_{s\perp}^2$. In other words, the dominant momenta of the virtual gluons come from the multi-Regge region, the same as those used in the dispersion-relation approach [5].

B. Crossed Ladders

When the rungs of the ladders are crossed, the scalar diagram will no longer be saturated. This could be inferred from the example above and the s-channel dispersion relation, but let us see how to obtain this conclusion directly from the Feynman diagram, and how unsaturated it is.

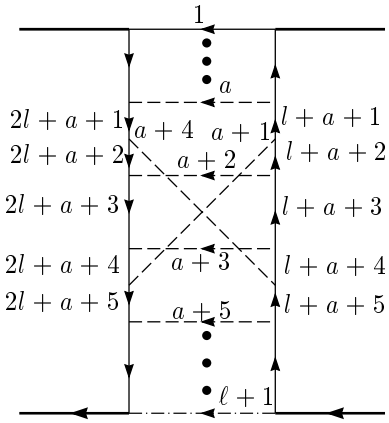

FIG. 7. A crossed ladder diagram, with path P given by the light solid line and the pole lines given by the dotted lines. The rungs above a and below $a + 5$ are all uncrossed.

Consider Fig. 7, which is obtained from Fig. 6 by crossing two rungs separated by $r = 2$ horizonatal rungs in between. The path P and the contributing pole remain unchanged. As before, we let $Q'_j = Q_j$ for $1 \le j \le a$, and let these Q'_j's to be strongly ordered as before. Then $m_j = 1$ just as in the previous example. The question is what happens when we come to the region where the rungs are crossed.

Every '+' momentum $q_{i+}\sqrt{s}$ $(1 \le i \le 3\ell + 1)$ is a linear combination of some a_p/Q_p $(2 \le p \le \ell + 1)$. We shall use the symbol $[p_1 p_2 \cdots p_k]$ to represent this '+' momentum if it receives contributions from $p = p_1, p_2, \cdots, p_k$ *in the crossed region*. Similarly, its '−' momenta are linear combinations of Q_1 and Q_p $(2 \le p \le \ell)$, and those from the crossed region that contribute to the '−' momentum of a particular line will be enclosed between angular brackets $\langle \cdots \rangle$.

The '−' and '+' momenta contributions for the side line $s = \ell + a + k$ on the right $(1 \le k \le 5)$ are $\langle a, \cdots, a + k - 1\rangle[a + k, \cdots, a + 5]$. For the side lines $s = 2\ell + a + k$ on the left, they are $\langle a\rangle[a + 4, a + 2, a + 3, a + 1, a + 5]$ for $k = 1$, $\langle a, a+4\rangle[a+2, a+3, a+1, a+5]$ for $k = 2$, $\langle a, a+4, a+2\rangle[a+3, a+1, a+5]$ for $k = 3$, $\langle a, a+4, a+2, a+3\rangle[a+1, a+5]$ for $k = 4$, and finally $\langle a, a + 4, a + 2, a + 3, a + 1\rangle[a + 5]$ for $k = 5$. There is no way to strongly order the variables $Q_{a+1}, Q_{a+2}, Q_{a+3}, Q_{a+4}$ in the crossed region to get rid of all the obstructions. Whatever that works on the right hand side will fail on the left hand side, and vice versa. The only way out is to have these four to be of the same order, for then the ratio of any two of these four would be of order 1, and all the obstructions from the side lines would disappear. Their common radial variable $Q'_{a+1} = (\sum_{i=1}^{4} Q_{a+i}^2)^{1/2}$ is singular, with $m_{a+1} = 1$, because $Q'^3_{a+1} dQ'_{a+1}/Q'^4_{a+1} = dQ'_{a+1}/Q'_{a+1}$. From there on, everything looks like the uncrossed ladder again, so $Q'_j = Q_{j+3}$ for $a + 2 \le j \le p = \ell - 3$. The final integral F is proportional to $(\ln s)^{\ell-3}$, hence unsaturated. More generally, the same argument shows that if there are r uncrossed rungs between the two crossed rungs, then $F \sim (\ln s)^{\ell-r-1}$.

C. Two-Loop QED Diagram

Consider now the two-loop diagram Fig. 1 for electron-electron scattering by exchanging 3 photons.

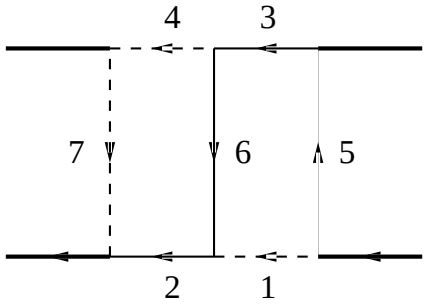

FIG. 8. The solid line is the path P' used to obtain the contributing poles from Fig. 1, indicated here by dotted lines. This is a different path than the one used in Fig. 3.

We shall compute this in two ways. First, using the path P and the contributing poles of Fig. 3, we will obtain saturated contributions from each of these two contributing poles, but their sum vanishes so this diagram turns out to be unsaturated. To see this unsaturation directly, we will use another path P' shown in Fig. 8. This path has only one contributing pole so there can be no chance of a cancellation, and it gives rise to an unsaturated LLA amplitude. In this latter approach we would also be able to compute the coefficient of the leading log term by LLA calculation if we should want to.

The numerator N of (6.1) in this case comes from the vertices, and is proportional to s. For simplicity we will assume it to be simply s.

The path P from Fig. 3 gives two contributing poles, $I_1 = (1, 2)$ and $I_2 = (1, 6)$. First consider $I_1 = (1, 2)$. Since both poles lie on the bottom line, $Q_1 \simeq Q_2 \simeq 1$, there are no obstructions on the side lines. Since $Q_3 > Q_4$, the integral is

$$\begin{aligned} F &\simeq -\frac{s}{a_5 a_6 a_7} \int_{(\xi/s} \frac{dQ_4}{Q_4} \int_{Q_4} \frac{dQ_3}{Q_3} \\ &\simeq \frac{s}{(-)^3 a_5 a_6 a_7} \int_{\xi/s} \frac{dQ_4}{Q_4} \int_{Q_4} \frac{dQ_3}{Q_3} \simeq -\frac{s}{2a_5 a_6 a_7} (\ln s)^2. \end{aligned}$$

(7.3)

Next consider $I_2 = (1, 6)$. The pole on 6 causes an obstruction from lines 2 and 7. By choosing $Q'_1 = Q_4 \ll Q'_2 = Q_6$, the obstruction from line 7 is removed but the obstruction from line 2 remains because $Q_2 \simeq 1$. However, since $Q_3 \simeq Q_6 = Q'_2$, the contribution from I_2 is

$$F \simeq \frac{s}{(-)^2 a_5 a_7} \int_{\xi/s} \frac{dQ'_1}{dQ'_1} \int_{B_1 Q'_1} \frac{dQ'_2}{Q'^2_2 (a_6/Q'_2)}$$
$$\simeq + \frac{s}{2a_5 a_6 a_7} (\ln s)^2. \tag{7.4}$$

The sum of the contributions from I_1 and I_2 vanishes in order $(\ln s)^2$ so the diagram is unsaturated.

To see this unsaturation directly, choose another path P' as shown in Fig. 8. The contributing pole is now $I' = (1, 7)$. The obstruction induced by line 7 on lines 2 and 6 block out the factor $d_4 d_7 = Q_4 Q_7$, so to get a singular integrand for F we must enlist the help of Q_3. If Q'_1 is the radial variable of Q_7 and Q_3, then the integrand of F is proportional to $Q'_1 dQ'_1/Q_3 Q_4 Q_7 d_2 \sim dQ'_1/Q'_1$, so the leading contribution to this diagram is of the order $\ln s$.

D. Four-Loop Diagram

If the path P for the four-loop diagram Fig. 2 is chosen as in Fig. 4, then as we have seen there are 10 contributing poles. For illustration we will look at the contribution from a single one, $(7, 3, 10, 2)$. We shall see that there will be no $\ln s$ enhancement if the diagram is scalar, but if it is a QCD diagram then there will be a linear $\ln s$ enhancement from this contributing pole.

There are two top lines in this diagram, lines 4 and 5. Since $Q_5 > Q_4 = Q_7$, the only single-variable candidate for Q'_1 is $Q_4 = Q_7$. However, the pole in 7 produces an obstruction on all the other lines in its natural loop: lines 8, 12, and 13. With three obstructing lines and only two singular factors, the resulting Q'_1 dependence cannot be singular for a scalar diagram. One could go on and try to find a singular Q'_1 among the radial variables of several Q_j's, and one would not succeed either. Consequently as a scalar diagram it has no $\ln s$ enhancement.

As a QCD diagram we must incorporate the vertex factors into the numerator N of the integrand of F. The vertex factor for a gluon connected to the top line is $2p_2$, and to the bottom line is $2p_1$. There are however also three triple-gluon vertices, at the junctions of lines $(6, 7, 13) = A, (11, 12, 13) = B$, and $(8, 10, 12) = C$. Each of them contains three terms, but one of the three terms of each is dotted into $2p_1$ and therefore produce an appropriate combinations of q_{i+}: $g_{7,13}(q_{7+} - q_{13+})$ for A, $g_{12,13}(q_{12+} + q_{13+})$ for B, and $g_{8,12}(q_{8+} + q_{12+})$ for C. Since every line in the natural loop of 7 contains $\pm q_{7+}$, and hence a factor $1/Q'_1$, these three vertex factors can make the Q'_1 variable much more singular. However, we may use only two out of the three, for otherwise the $g_{\alpha\beta}$ factors will lead to a dot product of the (7,4) vertex and the (4,5,8) vertex, thus producing an extra factor $2p_2 \cdot 2p_2 = 0$. With the help of two triple-gluon vertices, we get $m_1 = 1$ and a $\ln s$ enhancement from the Q'_1 variable.

The remaining singular factors for the integrand come- from lines 5 and 10. Since $Q_5 > Q_{10}$, if Q'_2 comes from a single variable Q_j we must have $j = 10$. This pole at 10 may produce obstructions on lines of its natural loop (10,12,13,6,1). Those on lines 12 and 13 have already been removed by Q'_1, so this leaves obstructions from lines 1 and 6. The one on 1 is particularly troublesome because it is a bottom line, so $Q_1 \simeq 1$ and the obstruction can never be removed. For that reason Q_{10} is not a singular variable, and it can be checked that the radial variable of Q_{10} and one or two other Q_j's cannot be a singular variable either. The enhancement of the QCD diagram is therefore just $\ln s$.

E. Nonabelian Cut Diagram

As a last example we consider the nonabelian cut diagram, Fig. 5, treated as a scalar diagram with numerator factor $N = 1$. The path is $P = (1, 5, 10, 6, 3)$ and the contributing poles are $(2, 7)$ and $(2, 9)$. Since in the LLA we would never have to consider any contributing pole on the top line, we can drop (2,9) and consider only (2,7).

In either case there is actually a hidden contributing pole at line 1. This does not show up explicitly in the path method because the cut line 8 reduces the flow diagram into a two-loop diagram, hence only two of the three poles show up explicitly. In any case, since $Q_4 = Q_8 = 0$, we have $Q_1 = 1$, so the pole at 1 produces $q_{1+} = a_1$. This together with the q_{p+} obtained from the other two pole lines uniquely determine all the '+' momenta of all the lines. However, the contribution from q_{1+} is finite, it will never lead to an obstruction, so in some sense we can just forget about it.

Of the two uncut top lines, $Q_{10} > Q_9 = Q_7$, so if Q'_1 is given by a single Q_j, it would have to be $j = 9$. The second singular variable is $Q'_2 = Q_6 = Q_{10} \gg Q'_1$, and the integral is

$$F = \int_{\xi/s} \frac{dQ'_1}{Q'^2_1(-a_7/Q'_1)(-a_6)} \int_{m_1 Q'_1} \frac{dQ'_2}{Q'_2(-a_5)(-a_4)} \int dQ_8(-2\pi i)\delta(Q_8) \simeq -\frac{\pi i}{a_4 a_5 a_6 a_7}(\ln s)^2. \tag{7.5}$$

VIII. ACKNOWLEDGEMENT

This research was supported in part by the Natural Science and Engineering Research Council of Canada and by the Québec Department of Education. Y.J.F. acknowledges the support of the Carl Reinhardt Major Foundation, and C.S.L. wants to thank Hung Cheng for a stimulating discussion.

---

† Electronic address: feng@physics.mcgill.ca
* Electronic address: lam@physics.mcgill.ca

[1] C.S. Lam, hep-ph/9804463.
[2] For example, see V.S. Fadin and L.N. Lipatov, *Nucl. Phys.* **B477** (1996) 767; hep-ph/9802290.
[3] R.J. Eden, P.V. Landshoff, D.I. Olive, and J.C. Polkinghorne, *The Analytic S-Matrix*, (Cambridge University Press, 1966).
[4] H. Cheng and T.T. Wu, *'Expanding Protons: Scattering at High Energies'*, (M.I.T. Press, 1987).
[5] L.N. Lipatov, Yad. Fiz. 23 (1976) 642 [Sov. J. Nucl. Phys. 23 (1976) 338]; Ya. Ya. Balitskii and L.N. Lipatov, Yad. Fiz. 28 (1978) 1597 [Sov. J. Nucl. Phys. 28 (1978) 822]; E.A. Kuraev, L.N. Lipatov, and V.S. Fadin, Zh. Eksp. Teor. Fiz. 71 (1976) 840 [Sov. Phys. JETP 44 (1976) 443]; *ibid.* 72 (1977) 377 [*ibid.* 45 (1977) 199]; V. Del Duca, hep-ph/9503226.
[6] J. Bartels, *Nucl. Phys.* **B151** (1979) 293; **B175** (1980) 365.
[7] H1 Collaboration, hep-ex 9708016; ZEUS Collaboration, hep-ex 9709021.
[8] J. Bartels, *Z. Phys.* **C60** (1993) 471; J. Bartels and M. Wuesthoff, *Z. Phys.* **C66** (1995) 157; M.A. Braun, *Nucl. Phys.* **B175** (1980) 365; *hep-ph*/9706373.
[9] See, for example, the references cited in Ref. [1].
[10] Y.J. Feng, O. Hamidi-Ravari, and C.S. Lam, *Phys. Rev. D* **54** (1996) 3114.
[11] Y.J. Feng and C.S. Lam, *Phys. Rev. D* **55** (1997) 4016.
[12] C.S. Lam and K.F. Liu, *Nucl. Phys.* **B483** (1997) 514; *Phys. Rev. Lett.* **79** (1997) 597.
[13] H. Verlinde and E. Verlinde, hep-th 9302104.
[14] L.N. Lipatov, *Nucl. Phys.* **B365** (1991) 614; R. Kirschner, L.N. Lipatov, and L. Szymanowski, *Nucl. Phys.* **B425** (1994) 579; *Phys. Rev. D* **51** (1995) 838.